NASA Technical Memorandum 82892

Effects of Processing and Dopant on Radiation Damage Removal in Silicon Solar Cells

I. Weinberg, H. W. Brandhorst, Jr., and C. K. Swartz
Lewis Research Center
Cleveland, Ohio

and

S. Mehta
Cleveland State University
Cleveland, Ohio

Prepared for the
Third European Symposium on Photovoltaic Generators in Space
cosponsored by the Royal Aircraft Establishment,
U.K. Department of Industry, and European Space Agency
Bath, United Kingdom, May 4–6, 1982

NASA

EFFECTS OF PROCESSING AND DOPANT ON RADIATION DAMAGE REMOVAL IN SILICON SOLAR CELLS

I. Weinberg, H. W. Brandhorst, Jr., C. K. Swartz, and S. Mehta*

National Aeronautics and Space Administration
Lewis Research Center
Cleveland, Ohio 44135

ABSTRACT

Gallium and boron doped silicon solar cells, processed by ion-implantation followed by either laser or furnace anneal were irradiated by 1 MeV electrons and their post-irradiation recovery by thermal annealing determined. During the post-irradiation anneal, gallium-doped cells prepared by both processes recovered more rapidly and exhibited none of the severe reverse annealing observed for similarly processed 2 ohm-cm boron doped cells. Ion-implanted furnace annealed 0.1 ohm-cm boron doped cells exhibited the lowest post-irradiation annealing temperatures (200° C) after irradiation to 5×10^{13} e^-/cm^2. The drastically lowered recovery temperature is attributed to the reduced oxygen and carbon content of the 0.1 ohm-cm cells. Analysis based on defect properties and annealing kinetics indicates that further reduction in annealing temperature should be attainable with further reduction in the silicon's carbon and/or divacancy content after irradiation.

E-1270

INTRODUCTION

It is well known that degradation due to particulate space radiation is the most significant factor in reducing solar cell output. One possible solution to the degradation problem lies in attaining the capability to periodically anneal and thus restore cell performance in space. However, the currently-used silicon solar cells undergo reverse annealing and require temperatures around 400° C in order to restore cell performance. At this latter temperature, irreversible damage to array components occurs. Temperatures around 200° C, or below, are required to prevent such damage. With respect to possible increases in radiation resistance, gallium-doped cells appear promising in contrast with cells whose p-dopant is boron (ref. 1). In the present case, our main interest lies in comparing the annealability of such cells. Because annealing of gallium-doped cells with diffused junctions has been previously investigated (ref. 2), we focus our attention on cells whose junctions are formed by phosphorus ion-implantation followed by either furnace or laser annealing to remove implant damage. These are compared to boron-doped cells prepared by identical processes from the same 2 ohm-cm starting material. Additional results are presented for cells fabricated from 0.1 ohm-cm boron doped silicon.

EXPERIMENTAL PROCEDURES

Irradiations and annealing were performed on n+p cells with 2 and 0.1 ohm-cm base resistivities. The 2 ohm-cm silicon cells were processed from vacuum float zone silicon whose boron doping was achieved by either

---

*NASA-Cleveland State University Intern.

introducing diborane gas during float zoning or implanting boron ions prior to the float zone operation (refs. 1 and 3). Gallium doping was achieved by introducing elemental gallium into the seed end of the rod prior to zone melting (ref. 1). Additional details concerning the 2 ohm-cm starting silicon are contained in reference 1 and the final report of the contract under which the material was prepared (ref. 4). The p-n junctions were formed by phosphorus ion implantation followed by either laser annealing or a multi-step furnace anneal (ref. 5). The 0.1 ohm-cm cells were processed from Wacker, Waso-S float zone, boron-doped silicon with the ion implantation step being followed by a furnace anneal to remove implant damage. Infrared absorption measurements determined that the gallium-doped 2 ohm-cm silicon had a carbon content of $2.5 \times 10^{16}/cm^3$ and an oxygen content $10^{17}/cm^3$ while the boron doped 0.1 ohm-cm silicon had oxygen and carbon concentrations $5 \times 10^{15}/cm^3$.

Phosphorus ions were implanted at energies of 10 KeV to a fluence of $2.5 \times 10^{15}/cm^2$ to form the n^+ cell regions. Laser annealing was performed at a wavelength of 0.532 micrometer using a Nd:YAG laser. The furnace anneal was a multistep process, carried out in nitrogen, in which the cells were heated at 550° C for 2 hours, then at 850° C for 15 minutes and finally at 550° C for 2 hours.

After processing and contact formation, the uncoated cells were irradiated by 1 MeV electrons to a fluence of $10^{15}/cm^2$. All cells were isochronally annealed in 50° C steps with time at temperature being 20 minutes. Isothermal anneals were performed at temperatures where the isochronal anneal indicated the possibility of significant low temperature annealing.

EXPERIMENTAL RESULTS

Isochronal annealing data for the 2 ohm-cm cells are shown in figures 1 and 2 while the same data for the 0.1 ohm-cm cells are shown in figure 3. Data are shown for the fluences of 5×10^{13} and $10^{15}/cm^2$. In each case, fluence dependencies are observed. With respect to degradation, the laser annealed gallium-doped cells showed the least degradation at both fluences. However, the effect was more pronounced at the lower fluence. For the furnace annealed cells, both the gallium-doped and diborane-doped cells showed the least degradation at the lower fluence. The 2 ohm-cm gallium-doped cells showed no reverse annealing while the remaining 2 ohm-cm cells exhibit the reverse annealing usually observed with boron-doped cells of this resistivity (ref. 6). The gallium-doped furnace annealed cells show full recovery on annealing at 350° C and a slightly higher recovery temperature for the similarly doped laser annealed cells. With the exception of the 2 ohm-cm, boron doped furnace annealed cells, the remaining cells show recovery at 400° C or higher. In contrast the 0.1 ohm-cm cells, (fig. 3), show no reverse annealing at both fluences (ref. 6) and a dramatically large reduction in annealing temperature at the lower fluence.

Thus, both the 2 ohm-cm gallium-doped and the 0.1 ohm-cm boron-doped cells, irradiated at the lower fluence, show evidences of some degree of damage recovery when isochronally annealed at temperatures below 300° C. Since our objective is to accomplish annealing temperatures of 200° C or lower, isothermal annealing was carried out at this temperature. After 15 hours, little or no recovery was observed in the gallium-doped furnace

annealed 2 ohm-cm cells at this temperature (fig. 4). A similar result was obtained with the gallium-doped laser annealled cells. On the other hand, the boron-doped 0.1 ohm-cm cells, irradiated at the lower fluence, showed substantial recovery when annealed at 200° C for 5 hours (fig. 5). This represents the lowest temperature for which recovery is observed when isothermally annealing boron-doped silicon solar cells.

DISCUSSION

Reverse Annealing

The reverse annealing observed in the 2 ohm-cm cells has been previously considered and attributed to a defect which was tentatively identified as a complex of boron, oxygen and a vacancy (ref. 6). For the gallium-doped cells, a detailed picture of defect complexes is not available; thus we are unable to relate the absence of reverse annealing to any defect or combination of defects at this time.

Low Temperature Annealing

Although a fluence dependent reduction in isochronal annealing temperature is noted for the gallium-doped, 2 ohm-cm silicon cells, the reduction is small when compared to the lowering of recovery temperature observed at the lower fluence in the isochronal annealing of the 0.1 ohm-cm boron-doped cells. The superior annealability of these latter cells is manifested in the recovery observed when isothermally annealed of 200° C. In this connection, it is noted that the carbon and oxygen content of the 2 ohm-cm cells is greater than that observed for the 0.1 ohm-cm cells.

Further insight into the reasons for the reduced annealing temperature can be gained from the behavior of the radiation induced defects during thermal annealing. At present, extensive information on such defect behavior is available for boron-doped but not for gallium-doped silicon. Hence, we restrict our consideration of defect behavior to the case of boron-doped silicon. In particular, our interest lies in identifying the defects which are removed by annealing at 300° C.

The temperatures at which major defects in boron-doped silicon appear and disappear during isochronal anneal are summarized in Table I. The defects were detected by Deep Level Transient Spectroscopy (DLTS) and/or Electron Paramagnetic Resonance (EPR). In the table, the defects are characterized by energy level and the temperature at which the defects appear and disappear during the isochronal anneal. Several of the defects are unidentified and there exists ambiguity with respect to defect identification. However, pertinent for the present case is the fact that only two of the possible defects shown anneal at 300° C. These are the carbon-carbon pair at E_V+0.38eV and the divacancy at E_V+0.23 eV. Hence, it is concluded that isochronal annealing (figure 3) removes either the divacancy and/or the carbon-carbon pair at 300° C. In order to investigate defect removal below 300°C, we have performed isothermal annealing at several points below this temperature (fig. 6). Using this data we find (Appendix A) that the activation energy for annealing is 1.5 ± 0.2 eV. This agrees within experimental error, with the activation energy for annealing of both the divacancy and carbon-carbon pair (Appendix A). This supports the conclusion

obtained from the data of Table I. It also suggests that reduction in annealing temperature below 200° C could be obtained by further reduction of the carbon and/or divacancy concentrations in silicon.

Effects of Processing

From the data presented here, for the 2 ohm-cm cells, whether furnace or laser annealed, the major difference in behavior between the gallium-doped and boron-(or diborane) doped cells is a small reduction in annealing temperature and the absence of reverse annealing. At the lower fluence, processing by furnace annealing appears to result in lower annealing temperature for all 2 ohm-cm cells.

The 0.1 ohm-cm cells show a rather dramatic drop in isochronal annealing temperature to 300° C at the lower fluence. Furthermore, isothermal annealing occurs at 200° C, a phenomenon which does not occur in the 2 ohm-cm cells. We note that all cells for which data are shown have had p-n junctions formed by ion-implantation. Thus, the major difference between the 0.1 ohm-cm and 2 ohm-cm cells is the lowered oxygen and carbon content exhibited by the lower resistivity cells.

CONCLUSION

From the results of the present study, for the 2 ohm-cm cells produced by ion-implantation and either furnace or laser annealing, it is concluded that:

Gallium-doping results in lower annealing temperatures and the absence of reverse annealing.

At low fluence ($5 \times 10^{13}/cm^2$), processing by furnace annealing yields a slightly lower isochronal annealing temperature.

The 2 ohm-cm cells show no recovery when isothermally annealed at 200° C

On the other hand, for the 0.1 ohm-cm cells, with reduced oxygen and carbon content, processed by ion-implantation and furnace annealing:

A 200° C reduction in isochronal annealing temperature is observed at the lower fluence.

Substantial recovery is achieved on isothermal annealing at 200° C.

The defects removed by annealing below 300° C are the divacancy and/or the carbon-carbon pair.

For both the 0.1 and 2 ohm-cm cells processed by ion-implantation, any process steps which result in reduced carbon and oxygen content in the starting silicon should lead to substantial damage removal by annealing below 300° C.

APPENDIX A - Activation Energies

The activation energy for annealing is obtained from the relation (ref. 13)

$$K = K_0 \exp(-E_A/k_bT) \quad (1)$$

where K is the reaction rate constant, E_A is the activation energy, T is the temperature and K_0 is a constant which is frequently taken to be equal to the maximum lattice vibrational frequency. If the annealing kinetics are second order, then;

$$\frac{N}{N_0} = \frac{1}{1 + KN_0t} \quad (2)$$

where N is the defect concentration at time t and N_0 the defect concentration at the beginning of the reaction. In lieu of defect concentrations we use diffusion lengths, a quantity which we routinely measure. Assuming the presence of one dominant defect, it follows that (ref. 14)

$$\frac{1}{L^2} - \frac{1}{L_0^2} = BN \quad (3)$$

where L_0 is the pre-irradiation diffusion length, L is the diffusion length at time t during the anneal and B is a constant at constant temperature. Hence from equations 2 and 3

$$\left(\frac{1}{L^2} - \frac{1}{L_0^2}\right)^{-1} = C + \frac{kt}{B} \quad (4)$$

where C is a constant

Plots of equation (4) for $\phi = 5\times10^{13}/cm^2$ are shown in figure 7 for T = 200, 250, 275, and 300° C. A similar straight line is obtained for 200° C. Because an attempt to fit the data to first order kinetics was unsuccessful, it follows that the annealing is reasonably described by second order kinetics.

Equation 1 can be rewritten as

$$\frac{K}{B} = \frac{K_0}{B} \exp\frac{-E_A}{k_bT} \quad (5)$$

A plot of equation 5 using the present data is shown in figure 8 from which, by a least squares fit, we obtain

$$E_A = 1.5 \pm 0.2 \text{ eV}$$

The activation energy for divacancy annealing is found to be 1.2 eV from infrared studies (ref. 15) while that obtained from EPR is 1.3 eV (ref. 11).

For the carbon-carbon pair the activation energy for defect re-orientation is found to be 1.2 eV from EPR studies (ref. 12). No activation energy for annealing is available for the carbon-carbon pair. However, the activation energy for atomic re-orientation has, in the case of divacancy, been found equal to that for annealing (ref. 15). If we assume this to be the case for the carbon-carbon pair, then the activation energy obtained from the current annealing kinetic studies is consistent with the presence of either the divacancy or the carbon pair below 300° C. The annealing process below 300° C is thus one in which either or both of these defects is annihilated with temperatures above 200° C being necessary to remove this defect in the present low resistivity silicon.

REFERENCES

1. Fodor, J.; and Opjorden, R.: Advanced Silicon Material for Space Solar Cells, 14th IEEE Photovoltaic Specialists Conference, San Diego 7-10 Jan. 1980, 882-886.

2. Scott-Monck, J. A.; and Anspaugh, B. E.: Effect of Dopants on Annealing Performance of Silicon Solar Cells, Conference on Solar Cell High Efficiency and Radiation Damage, NASA Conference Publication 2097, 1979, 173-183.

3. The 2 ohm-cm wafers were supplied by Dr. Patrick Rahilly of the Aero Propulsion Lab., Wright Patterson Air Force Base, Ohio, U.S.A.

4. AFWAL-TR-81-2013 (Wright-Patterson AFB) 1981, Low Resistivity-High Lifetime Single Crystal Silicon Investigation, by Fodor, J.; and Opjarden, R. W.

5. The ion-implantation and subsequent anneal, to remove implant damage, were performed by the Spire Corporation, Bedford, Massachusetts, U.S.A.

6. Weinberg, I.; and Swartz, C. K.: Origin of Reverse Annealing in Radiation-Damaged Silicon Solar Cells, Appl. Phys. Lett. 36, 1980, 693-695.

7. Mooney, P. M.; et al.: Defect Energy Levels in Boron-Doped Silicon Irradiated with 1-MeV Electrons, Phys. Rev. B: Solid State 15(8), 1977, 3836-3843.

8. Lee, Y. H.; et al.: EPR of a Carbon-Oxygen-Divacancy Complex in Irradiated Silicon, Phys. Status Solidi, A 41(2), 1973, 637-647.

9. Brower, K. L.: EPR of a Jahn-Teller Distorted 111 Carbon Interstitial in Irradiated Silion, Phys. Rev. B: Solid State 9, 1973, 2607-2617.

10. Kimerling, L. C.: Defect States in Electron Bombarded Silicon: Capacitance Transient Analyses, Radiation Effects in Semiconductors, Dubrovnik 6-9 Sept. 1976, Conference Series - Institute of Physics, no. 31, 1973, 221-230.

11. Watkins, G. D.; and Corbett, J. W.: Defects in Irradiated Silicon: Electron Paramagnetic Resonance of the Divacancy, Phys. Rev. 138(2), 1965, 543-555.

12. Brower, K. L.: EPR of a 001 Si Interstitial Complex in Irradiated Silicon, Phys. Rev. B: Solid State, 14(3), 1976, 872-883.

13. Corbett, J. W.: Electron Radiation Damage in Semiconductors and Metals, New York, Academic Press, 1966, 36-43.

14. Shockley, W.; and Read, W. T., Jr.: Statistics of the Recombinations of Holes and Electrons, Phys. Rev. 87(5), 1952, 835-841.

15. Cheng, L. J.; et al.: 1.8-, 3.3-, and 3.9-Micron Bands in Irradiated Silicon: Correlations with the Divacancy, Phys. Rev. 152(2), 1966, 761-774.

TABLE I - ANNEALING TEMPERATURES OF MAJOR DEFECTS IN BORON-DOPED SILICON

Energy level, eV	Defect	Annealing temperature, °C		Detection method
		In	Out	
$E_v + 0.38$	V-O-C	<30	400	EPR[9], DLTS[6]
	or			
	C_I-C_S	<30	300	EPR[10], DLTS[11]
$E_v + 0.23$	Divacancy	<30	300	EPR[12], DLTS[6,11]
$E_c - 0.27$	B_I-O_I	<30	200	DLTS[6]
	or			
	B_I-B_S	<30	180	DLTS[11]
$E_v + 0.30$	B-O-V	100	400+	DLTS[6]
	or			
	S_I-S_I	200	500	EPR[13], DLTS[11]
$E_v + 0.26$	----------	270	400	DLTS[6]
$E_v + 0.43$	----------	<30	200	DLTS[6]

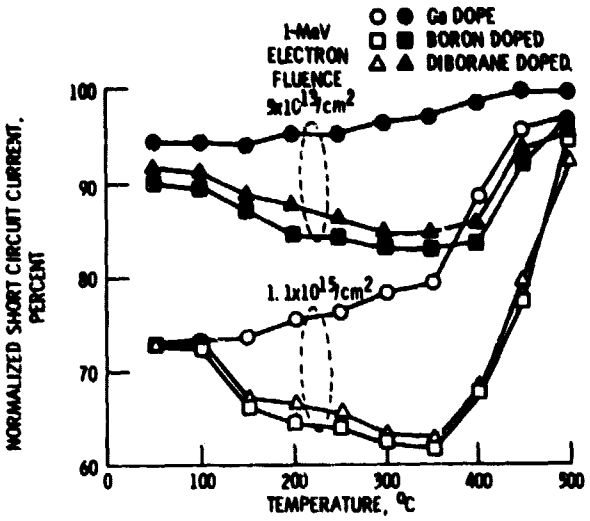

Figure 1. - Isochronal anneal of 2 ohm-cm ion-implanted, laser annealed cells.

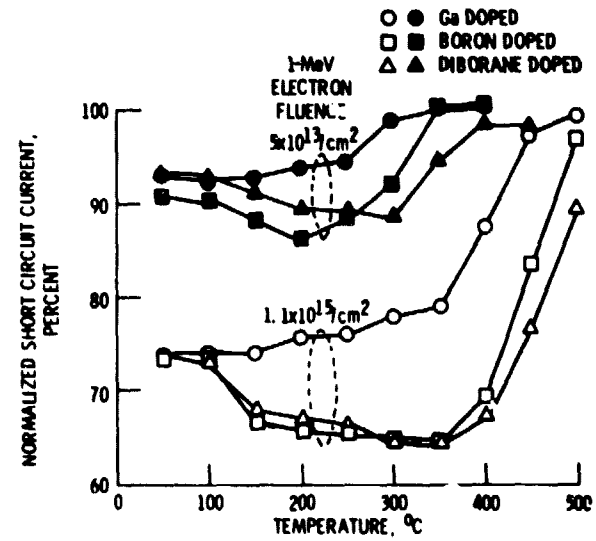

Figure 2. - Isochronal anneal of 2 ohm-cm ion-implanted, furnace annealed cells.

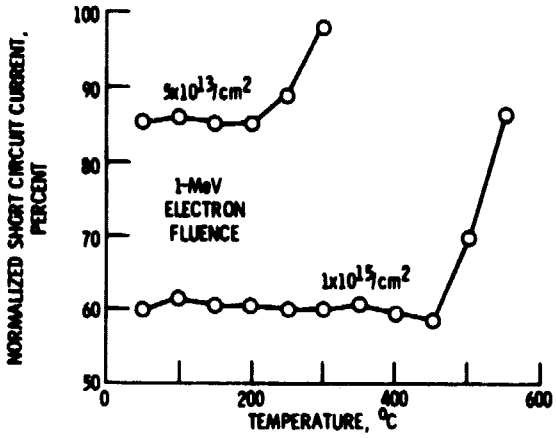

Figure 3. - Isochronal anneal of 0.1 ohm-cm ion-implanted, furnace annealed cells.

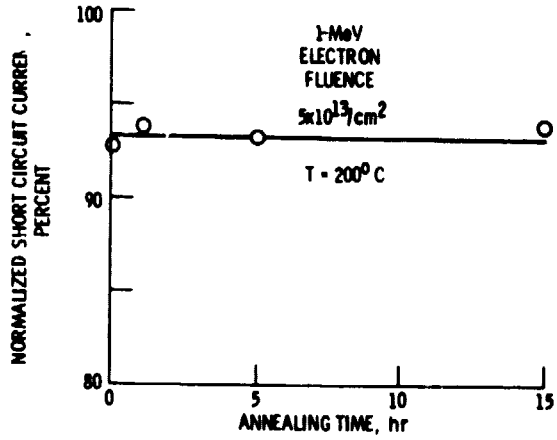

Figure 4. - Isothermal anneal of 2 ohm-cm Ga doped, ion-implanted, furnace annealed cell.

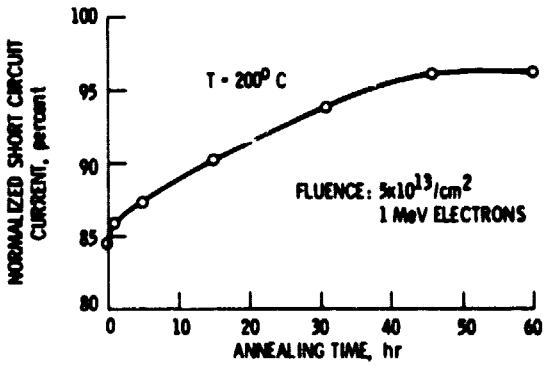

Figure 5. - Isothermal annealing at 200° C of 0.1 Ω-cm ion-implanted cell.

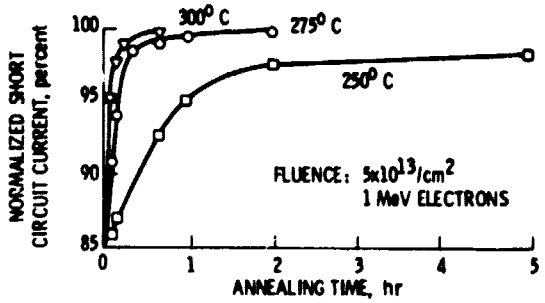

Figure 6. - Isothermal annealing of ion-implanted 0.1 Ω-cm cells.